2021 IEEE International Conference on Acoustics, Speech and Signal Processing

- My name is Teresa White
- Graduate student from the Department of Mathematics and Statistics at Utah State University

GPS-Denied Navigation Using SAR Images and Neural Networks

Teresa White[1], Jesse Wheeler[2], Colton Lindstrom[3], Randall Christensen[3], Kevin R. Moon[1]

[1]Dept. Mathematics & Statistics—Utah State University
[3]Dept. Electrical & Computer Engineering—Utah State University
[2]Dept. Statistics—University of Michigan

IEEE ICASSP 2021

June 6-11, 2021

** This research was partially supported by Sandia National Labs on grants 201782, 202136, and 202854. The support and resources from the Center for High Performance Computing at the University of Utah are gratefully acknowledged.*

GPS-Denied Navigation

Unmanned Aerial Vehicles (UAV) applications:

- Civil: Search and rescue operations,
- Commercial: Agriculture
- Aerospace: Aircraft maintenance
- Military: Aerial targets for combat training of human pilots

GPS-Denied Navigation

Precise navigation data is necessary for autonomous vehicles:

- Normal circumstances: GPS is typically used
- Abnormal circumstances: GPS signal may be denied
- Synthetic aperture radar (SAR) is used to provide the lost information in GPS-denied environments.
- Radar is independent of lighting or weather conditions.

SAR Images

- Back-projection Algorithm (BPA) is a technique for producing SAR images (Zaugg, 2015).
- SAR images are created by sending a series of radar pulses along the flight path that is assumed to be known.
- Inaccurate flight trajectory implies corrupted SAR images.

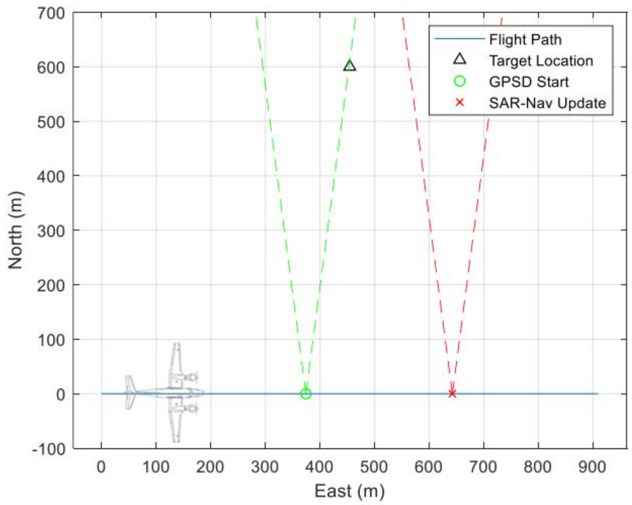

Proposed Method

- **Approach**: use a neural network to estimate the flight trajectory from distorted SAR images
  - Compare distorted images with a reference image
- **Result**: a large convolutional neural network (CNN) combined with transfer learning is able to learn the flight trajectory under different settings.

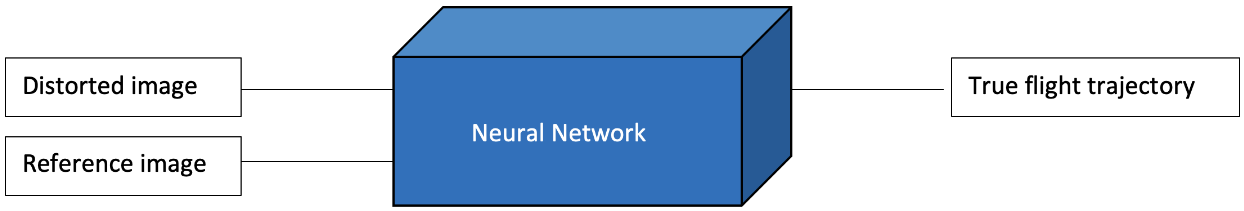

Background

Inertial Navigation

- Truth state vector:
$$x = \begin{bmatrix} \boldsymbol{p}^n & \boldsymbol{v}^n & q_b^n \end{bmatrix}^T$$
- Navigation state vector:
$$x = \begin{bmatrix} \hat{\boldsymbol{p}}^n & \hat{\boldsymbol{v}}^n & \hat{q}_b^n \end{bmatrix}^T$$
- Error state vector:
$$x = \begin{bmatrix} \delta \boldsymbol{p}^n & \delta \boldsymbol{v}^n & \delta \boldsymbol{\theta}^n \end{bmatrix}^T$$

Initial Errors

- **Key idea**: given an **initial condition for the navigation errors**, the true navigation states can be recovered.
- The task of correcting errors in the estimated trajectory is reduced to **determining the nine errors at the beginning of the time interval of interest** (*Christensen*, 2019).

Distortions from Navigation Errors

Error	Shift Direction	Blur Direction
AT Position	AT	None
CT Position	CT	None
D Position	CT	None
AT Velocity	None	AT
CT Velocity	AT	None
D Velocity	AT	None
AT Attitude	None	Small AT
CT Attitude	None	Small AT
D Attitude	None	Small AT

Table: Effect of navigation errors on BPA-SAR images.

Distortions from Navigation Errors

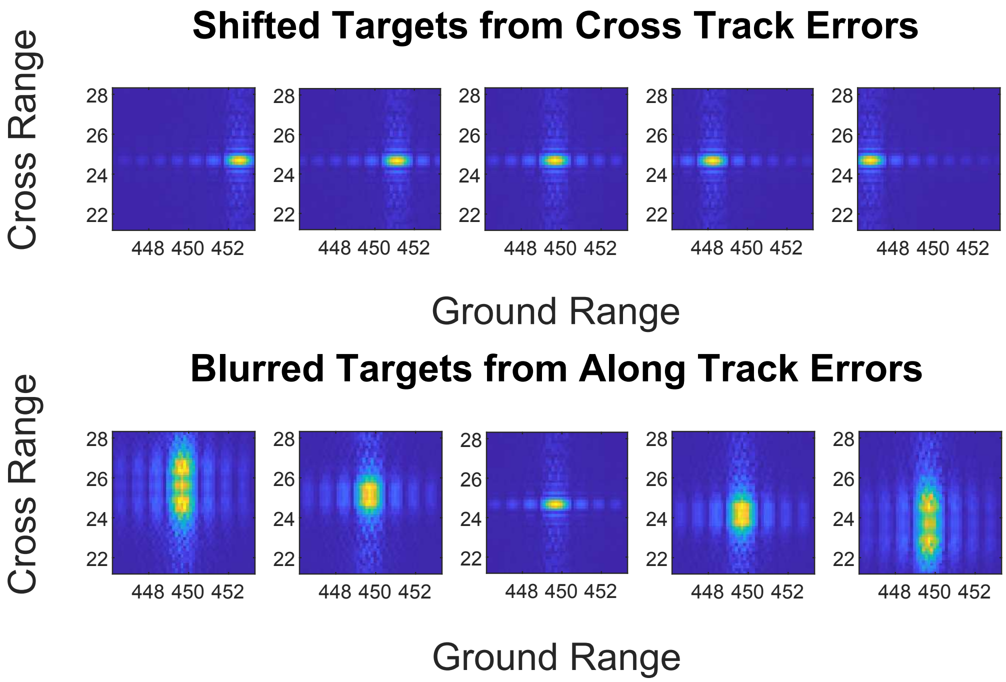

Figure: Demonstration of shifting and blurring distortions due to navigation errors.

The SAR Data

Three different sets of SAR image data:

- Simulated data with a 5 second aperture length (MATLAB)
- Two real datasets with a 2 and a 10 second aperture lengths (Space Dynamics Laboratory X-band radar system)

Scenarios

For each of the datasets, six different scenarios were studied

Scenario #	AT Pos	CT Pos	D Pos	AT Vel	CT Vel	D Vel
1	x	x				
2				x	x	
3	x	x		x	x	
4	x	x	x			
5				x	x	x
6	x	x	x	x	x	x

Table: Summary of scenarios and corresponding initial errors.

Data Splitting

Dataset	Training		Validation		Testing	
	# targets	# images	# targets	# images	# targets	# images
Sim-5-sec	134	13500	19	1900	39	3800
Real-2-sec	130	13000	18	1800	37	3700
Real-10-sec	122	12300	17	1700	36	3500

Table: Data split details: Training (70%), validation (10%), test (20%) set.

- Navigational errors are standardized to account for different scales.

Neural Network Approaches

- Advanced, pretrained network architectures were considered:
  - ResNet 18
  - ResNet 34
  - ResNet 50
  - ResNet 101
  - ResNet 152
  - Wide ResNet 50_2
  - Wide ResNet 101_2
- Wide ResNet 50_2 network outperformed all other models.
  - Suggests that transfer learning is helpful here

Neural Network Inputs

Our model:

- Input (3-channel image): Stacking the distorted image, the reference image, and the difference image.

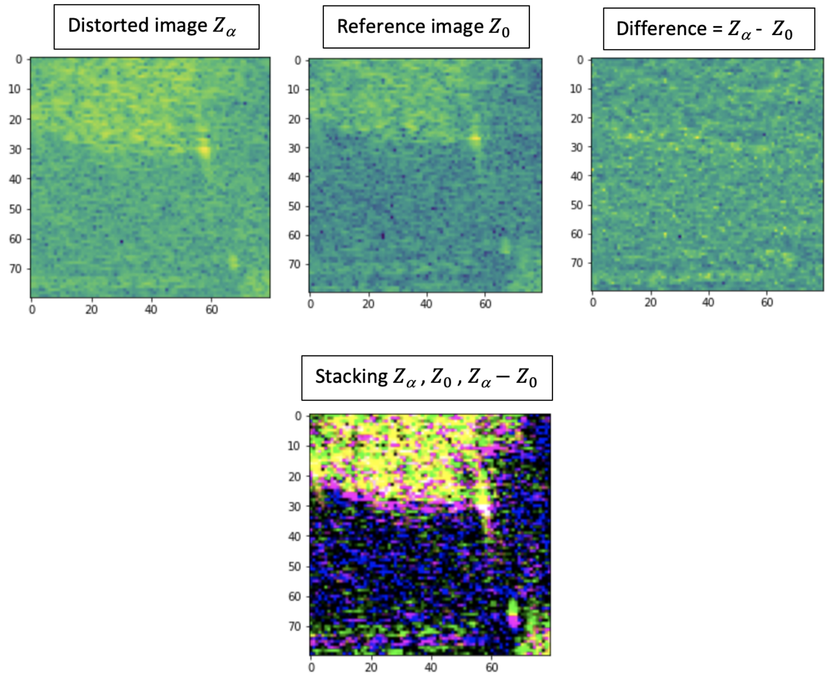

Neural Network Architecture

- This is fed into a randomly initialized convolutional layer followed by the ResNet architecture.
- The final layer of ResNet is replaced with a fully connected layer with the same number of outputs as error states.

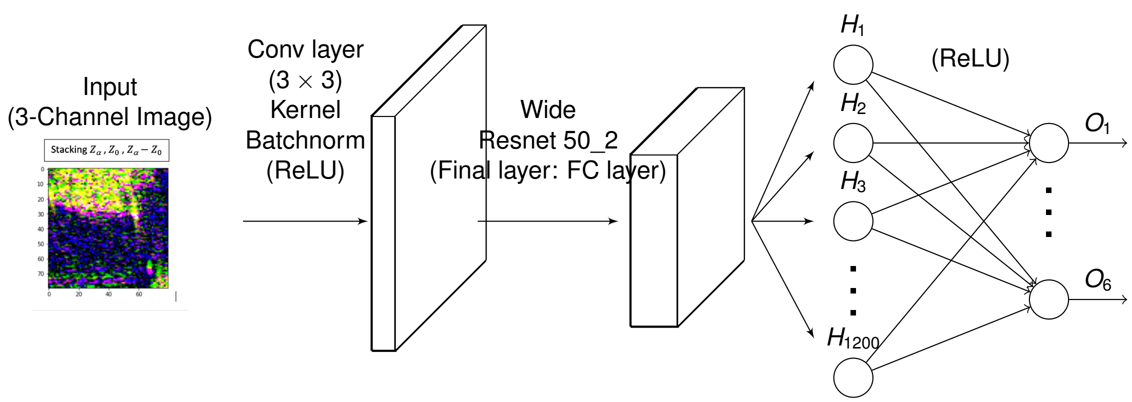

Loss Function

- We used the average mean squared error (MSE) loss function.

$$\text{MSE} = \frac{1}{mn}\sum_{\alpha=1}^{n}\sum_{\beta=1}^{m}\left(s_{\alpha_\beta} - \hat{s}_{\alpha_\beta}\right)^2,$$

[n] : Number of training images in the data
[m] : Number of error states considered
[s_{α_β}] : True standardized error of the βth error and the αth image
[$\hat{s}_{\alpha_\beta}$] : Corresponding error estimate by the neural network

- MSE less than one indicates that the neural network is learning relevant information for this task.
- We also used L2 regularization.

Experimental Results

Scenario #	Dataset	AT Pos	CT Pos	D Pos	AT Vel	CT Vel	D Vel
1	MSE (Sim-5-sec)	0.0594	0.0289	N/A	N/A	N/A	N/A
	MSE (Real-2-sec)	0.0563	0.0425	N/A	N/A	N/A	N/A
	MSE (Real-10-sec)	0.1808	0.1338	N/A	N/A	N/A	N/A
2	MSE (Sim-5-sec)	N/A	N/A	N/A	0.2456	0.1162	N/A
	MSE (Real-2-sec)	N/A	N/A	N/A	1.0729	0.1683	N/A
	MSE (Real-10-sec)	N/A	N/A	N/A	0.7895	0.0812	N/A
3	MSE (Sim-5-sec)	0.5229	0.2237	N/A	0.2442	0.1259	N/A
	MSE (Real-2-sec)	1.0657	0.2340	N/A	1.0682	0.1468	N/A
	MSE (Real-10-sec)	0.8864	0.2924	N/A	0.7894	0.1319	N/A
4	MSE (Sim-5-sec)	0.0941	0.9204	0.2800	N/A	N/A	N/A
	MSE (Real-2-sec)	0.1020	0.8102	0.3734	N/A	N/A	N/A
	MSE (Real-10-sec)	0.2694	0.8165	0.4186	N/A	N/A	N/A
5	MSE (Sim-5-sec)	N/A	N/A	N/A	0.2834	0.7982	0.5460
	MSE (Real-2-sec)	N/A	N/A	N/A	1.0699	0.6459	0.5795
	MSE (Real-10-sec)	N/A	N/A	N/A	0.9072	0.6453	0.5781
6	MSE (Sim-5-sec)	0.6321	0.9139	0.5245	0.3677	0.8661	0.5331
	MSE (Real-2-sec)	1.0846	0.7509	0.5353	1.0868	0.6039	0.5984
	MSE (Real-10-sec)	0.9875	0.7382	0.5102	0.9447	0.6233	0.5113

Table: Summary of Model Performance for each error state for scenarios 1-6 of the sim-5-sec, the real-2-sec and the real-10-sec datasets.

Experimental Results

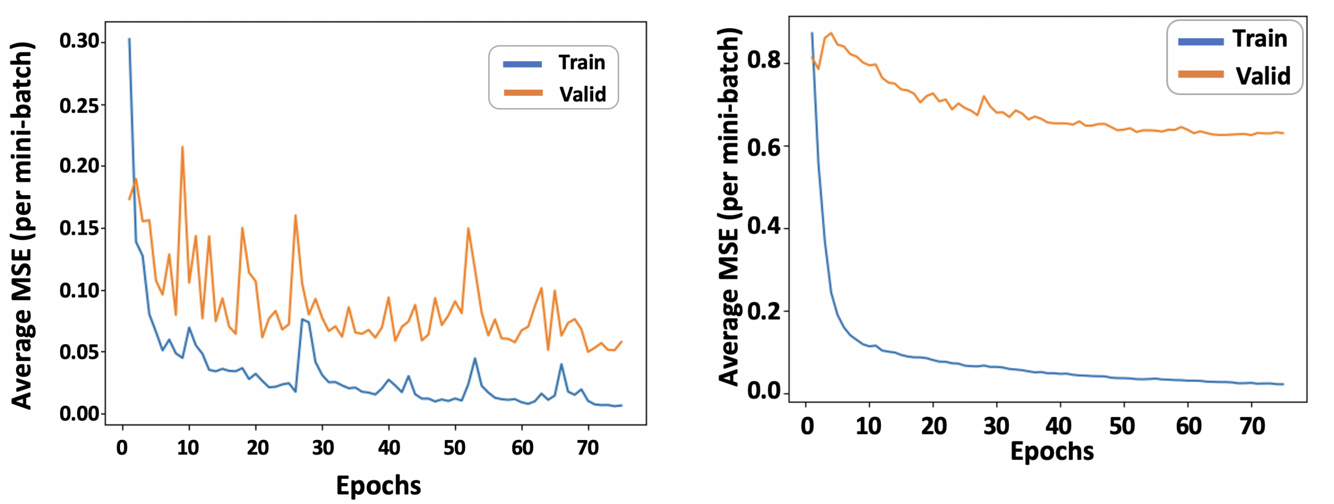

Figure: Training and validation MSE as a function of training epoch for scenario 1 and 2 (real-2-sec dataset).

Experimental Results

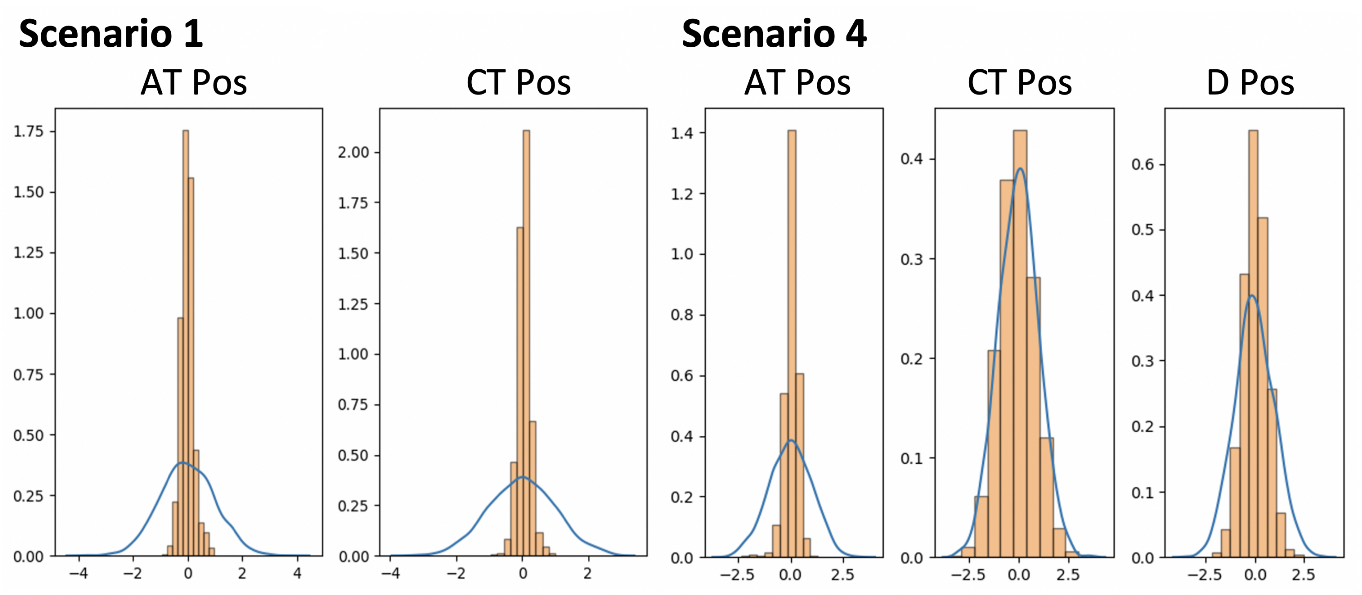

Figure: Distribution of Error States before (blue line) and after (histogram) estimation for the real-2-sec dataset for scenarios 1 and 4.

Conclusion

- We used a CNN to estimate position and velocity errors at the beginning of a SAR data collection period, by comparing a distorted SAR image with a SAR reference image.
- The network performs well in the absence of ambiguous error sources, reducing the MSE of the active navigation errors
- The network successfully distinguished between CT shifts caused by CT and D position errors.
- Increasing aperture length improves performance with blur-related errors.

Future Work

Possible future directions include:

- More research on the effect of the aperture length.
- More training data in future iterations will likely help mitigate overfitting.
- Augment the training data with information about the viewing geometry, including the estimated vehicle position at the beginning/end of the synthetic aperture

References

R. S. Christensen, J. Gunther, and D. Long, "Toward gps- denied navigation utilizing back projection-based synthetic aperture radar imagery," in *Proceedings of the ION 2019 Pacific PNT Meeting*, 2019, pp. 108-119.

C. Lindstrom, R. Christensen, and J. Gunther, "Sensitivity of bpa sar image formation to initial position, velocity, and attitude navigation errors," *arXiv*, vol. abs/2009.10210, 2020.

E. C. Zaugg and D. G. Long, "Generalized Frequency Scal- ing and Backprojection for LFM-CW SAR Processing," *IEEE Trans. Geosci. Remote Sens*, vol. 53, no. 7, pp. 3600-3614, July 2015.

THANK YOU!